Engineering Science and Technology, an International Journal xxx (xxxx) xxx

HOSTED BY

ELSEVIER

Contents lists available at ScienceDirect

Engineering Science and Technology, an International Journal

journal homepage: www.elsevier.com/locate/jestch

Full Length Article

Design and performance analyses of a fixed wing battery VTOL UAV

Özgür Dündar, Mesut Bilici *, Tarık Ünler

Necmettin Erbakan University, Faculty of Aeronautics and Aerospace, Aerospace Engineering Department, 42090 Meram, Konya, Turkey

ARTICLE INFO

Article history:
Received 27 July 2019
Revised 24 January 2020
Accepted 9 February 2020
Available online xxxx

Keywords:
VTOL
Battery powered UAV
Aerodynamic design
Performance calculations
Maximum endurance

ABSTRACT

The objective of this paper is to explain the design steps and performance analyses including energy consumption of a fixed-wing (FW) vertical take-off and landing (VTOL) unmanned air vehicle (UAV). The vehicle is designed from the beginning with the goal for low take-off weight and high aerodynamic performance. Aerodynamic design steps and sizing of both wing and control surfaces are demonstrated and static stability is fulfilled by evaluating the center of gravity location with respect to neutral point. In addition, power requirements and energy consumptions for take-off, climbing, cruise and landing are evaluated in perspective of flight performances to find out the required endurance for each flight condition. In order to do that selected battery is modelled in Simulink and results are represented. In take-off and landing flight conditions, momentum theory is implemented for vertical flight while the cruise flight is utilized to find out the maximum endurance. Drag calculations in level flight are performed in detail to experience the drawbacks of multi-rotor system including propellers providing vertical flight. Finally, VTOL-FW concept having multi-rotor system with four extra propellers and only fixed wing (FW) concept are compared in terms of endurance. It is found that FW concept without multi-rotor system with four propellers have much more endurance compared to VTOL-FW concept. Manufacturing with three-dimensional printers and flight tests of VTOL-FW UAV will be performed as a future work.

1. Introduction

Aerial vehicles have proved their capability in both military field such as patrolling, surveillance as well as reconnaissance, and civil areas including transport, rescue and agriculture of various applications over a hundred years, while enhancing their capabilities over time, and fulfilling ever-changing mission requirements. By means of smaller, safer and lighter platforms, UAVs propose an exclusive set of advantages compared to piloted aircrafts. Military and civil operations are the main areas where these advantages are effectively utilized. In addition, future UAVs are expected to perform much more extended missions with higher aerodynamic performance and higher degrees of automatic flight.

There are two prominent categories of mini UAVs; fixed-wing UAVs and multi-rotors. Fixed-wing UAVs are mini UAVs with propelled electrical batteries with longer ranges than UAVs with similar sizes of multi-rotor systems that require a runway or launcher for landing and knockout. On the other hand, the multi-rotor UAVs have rotor systems generally carrying three or four propellers that are capable of vertical take-off and landing (VTOL) and hovering over an area while carrying sufficient payload. In addition, they are more maneuverable than fixed wing UAVs with the ability of quickly transition from hover to cruise flight. However, the horizontally mounted rotor system is placed at the wings or the body that results in an enormous increase in drag force opposing the cruise flight. As a result of this decrement in the aerodynamic performance, fixed wing UAVs are more logical to be used to fulfill the missions needed high speed, long range and endurance flight [1]. The fixed-wing UAVs has longer flight time and duration, but it is not simple to secure a safe landing space, especially in the city and rugged train areas [2]. VTOL systems make more sense in operations such as mountainous and rural areas where there is no landing and take-off runway. In addition, VTOL systems must be used to operate like a helicopter in the required tasks such as hovering. However, if endurance is of first priority then a fixed wing type will most likely be preferred due to the efficiency of the cruise flight. If both of these features are demanded in a single operation then a fixed wing vertical and take-off landing (VTOL-FW) with level flight capability becomes the best option.

In order to combine the advantages of fixed wing aircraft and multi-rotor UAVs, hybrid UAV can be generated which is categorized into two main type, convertiplane and tail-sitter [3]. A convertiplane is classified into four subtypes, including tilt-rotor,

* Corresponding author.
E-mail address: mbilici@erbakan.edu.tr (M. Bilici).
Peer review under responsibility of Karabuk University.

https://doi.org/10.1016/j.jestch.2020.02.002
2215-0986/

Nomenclature

W_{TO}	total take-off weight
W_e	empty weight
W	weight
L	lift
D	drag
V	speed
S	area of wing
C_L	lift coefficient
C_D	drag coefficient
ρ_{SL}	sea level density
ρ_∞	density
V_∞	freestream velocity
q_∞	dynamic pressure
$C_{l,design}$	design lift coefficient
$C_{l,max}$	maximum lift coefficient of airfoil
$C_{L,max}$	maximum lift coefficient of whole UAV
S_{wing}	wing area
S_{ref}	wing area
S_{wet}	wetted area
Re	Reynolds number
W/S	wing loading
l	body length
b	wing span
AR	aspect ratio
V_{cruise}	cruise speed
V_{stall}	stall speed
$\Lambda_{c/4}$	quarter chord sweep angle
c_r	root chord
c_t	tip chord
λ	taper ratio
V_{HT}	horizontal tail volume ratio
V_{VT}	vertical tail volume ratio
l_{HT}	horizontal tail moment arm
l_{VT}	vertical tail moment arm
S_{HT}	horizontal tail wing area
S_{VT}	vertical tail wing area
$\bar{c}$	mean aerodynamic chord
C_l	airfoil lift coefficient
V_{max}	maximum speed
e	span efficiency factor
C_{D_0}	parasite drag coefficient
C_{D_i}	induced drag coefficient
$C_{f,\text{turbulent}}$	turbulent skin friction coefficient
K	aerodynamic factor
C_{fi}	skin friction coefficient
FF_i	drag calculation factor (form factor)
$S_{wet,i}$	wetted area
$S_{ref,i}$	reference area
$C_{D_{MR}}$	multi-rotor drag coefficient
$C_{0.7R}$	drag coefficient of 0.7 length propeller
M	Mach number
f	reference length
t	airfoil thickness
c	wing chord length
$(x/c)_m$	maximum thickness location
Λ_m	sweep angle
A_{max}	maximum area of body section
d	maximum radius of body section
N	number of vertical propellers
D	diameter of vertical propeller
P_{max}	maximum power
T_{TO}	take-off thrust
V_{TO}	take-off speed
K_T	ratio of thrust to weight
P_{TO}	power required for take-off
FM	figure of merit
A_{prop}	propeller area
φ	climb angle
V_{climb}	climb speed
P_{cruise}	power required for cruise
$P_{landing}$	power required for landing
P_{climb}	power required for climb
V_H	hover velocity
T_{hover}	hover power
T_{cruise}	cruise thrust
V_i	induced velocity
K	correction factor
V_{Des}	descent velocity
η_{cruise}	cruise condition efficiency
η_{prop}	propeller efficiency
η_{motor}	motor efficiency
η_{esc}	ESC efficiency
$\eta_{multirotor}$	multi-rotor system efficiency
$E_{range_{fw}}$	endurance of fixed wing portion
E_{range_mr}	endurance of multi-rotor system

tilt-wing, rotor-wing and dual system. Tilt-wing system features a wing that is horizontal for conventional forward flight and rotates up for vertical take-off and landing. It is similar to the tilt-rotor design where only the propeller and engine rotate. The advantage of tilt-rotor and tilt-wing is achieved by using their motor effectively because motors are utilized for both vertical and horizontal flight [4]. However, motor or wing tilting mechanism require complicated software as well as hardware such as inserting extra servo motors so that it both increases the drag and total weight of the vehicle. Stability during vertical take-off and transition is a critical point which may lead to the catastrophe. Najm et al. designed the complete nonlinear model of the six degree of freedom (6-DOF) UAV is adopted with the aim of designing a nonlinear PID (proportional integral derivative) controller for the stabilization [5]. In addition, Ozdemir et al. studied the design of a commercial hybrid VTOL UAV system to present that stability of the UAV is extremely complicated in transition flight [6]. Different types of fixed wing VTOL UAV designs [7] were also performed by Seunghee Yu et al. A tail-sitter is able to take-off and land vertically on its tail with the nose and thrust direction pointing upwards, and for fast forward flight the vehicle tilts to a near-horizontal attitude resulting in a more efficient lift production with conventional wings [8]. Transition from vertical to horizontal flight and vice versa are performed by its control surfaces or motors. This concept is reasonable for reducing the weight from the tilting or dual system, however, stronger and therefore complicated tails are required. Since its body is oriented vertically during VTOL mode, tail-sitter is more vulnerable to the wind. Consequently, complicated control system is necessary, such as VertiKUL [9], ITU Tail-sitter [10]. On the other hand, aerodynamic interaction between hover and the cruise flight is another handicap in VTOL-FW system. Droandi et al. [11] showed that the aerodynamic interactions between the wing and the rotor in hover for a scaled tilt wing aircraft half-span model. Aerodynamic effect of propeller-induced airstream which is a function of cruise speed, tilt angle and angle of attack changes the direction of local velocity [1]. Although several studies in VTOL-FW design and stability analyses are successfully implemented on different platform types, performance analyses and energy

Please cite this article as: Ö. Dündar, M. Bilici and T. Ünler, Design and performance analyses of a fixed wing battery VTOL UAV, Engineering Science and Technology, an International Journal, https://doi.org/10.1016/j.jestch.2020.02.002

consumption effect on battery and endurance in every flight modes have not been examined in detail.

In this study, a new VTOL-FW named Kuzgun with fixed wings and horizontally mounted rotor systems having four motor and propellers without tilt mechanism are designed and performance analyses are evaluated in terms of endurance by simulating Lithium-Polymer (Li-Po) battery. First of all, mission requirements and demands are determined for the selection of design methods. The competitors around the world are searched and listed in terms of geometric specifications and aerodynamic considerations. In the light of these search, some parameters are estimated including aspect ratio and wing surface area while others are calculated. Wing and control surfaces sizing are performed by using aerodynamic calculations [12,13]. After the conceptual design of VTOL-FW, flight performance calculations and energy consumptions are done for take-off, climbing, hovering and landing [14]. The battery model with the identified parameters are integrated in Simulink model and energy consumption is presented for every flight condition. In addition, by virtue of stability analyses, center of pressure values for different flight regimes are checked to ensure that it is in front of neutral point according to the nose of the UAV. It is evaluated that transition from hover to cruise flight consumes much energy of battery so that the engines and its mechanics contributed drag force substantially. It is concluded that the energy consumption of multi-rotors reduce the total endurance of VTOL-FW UAV unexpectedly.

2. Background and requirements

Even if civilian UAVs currently constitute 3% of total UAV market today, it is estimated that they will suggest 10% within the next years [15]. Although they are basically used in the field of military applications UAVs bring minimal risk and cost advantage to remarkable civilian applications which have once been considered as risky and costly due to the need for using manned air vehicles. Although VTOL-FW UAVs have less application area compared to all UAVs their market in Europe is expected to represent a continuous upward trend [16].

Most of the civilian UAV applications require UAVs that are capable of doing a wide range of different and complementary operations as a part of a composite mission. These operations include taking off and landing from limited runway space, while traversing the operation region in considerable cruise speed for mobile tracking applications. This is in addition to being able traverse in low cruise speeds or being able to hover for stationary measurements and tracking. All of these call for design features that provide supplementary but operation wise different capabilities. In addition, such a UAV system needs to be cost-efficient while providing easy payload conversion for different civilian applications. In this paper, preliminary design process of such a capable civilian VTOL-FW UAV system, namely the Kuzgun having the following primary features are performed:

- Vertical take-off and landing, and hovering at least 3 min,
- Relatively high cruise speed of 72 km/h,
- Endurance is at least 15 min,
- Payload is 700 g.

Before the VTOL-FW UAV design, which will meet the abovementioned requirements, mini VTOL-FW UAVs worldwide have been researched and presented in Table 1 together with some features to allow estimation of some design parameters and provide information about the overall concept of the design.

The wing area and span ratio information of the worldwide mini VTOL-FW UAVs in Table 1 are utilized as preliminary estimates in the wing and stabilizer design stage of the Kuzgun. In addition, the total take-off weight, payload and endurance information of competitors are used as a comparison of the concept design to ensure that the design is reasonable.

3. Design methodology

The design methodology of Kuzgun is presented at Fig. 1. Similar UAV systems are taken into account by considering mission and design requirements. Since the take-off weight is the most dominant parameter affecting the design, it is primarily crucial to estimate it. Sizing process is repeated iteratively according to weight in accordance with selected aerodynamic analyses. After that some critical performance parameters are calculated and compared to standard models by simulating in Simulink. Finally, sizing of wing and control surfaces are performed and properties of the wing and stabilizers are evaluated in the light of fulfilling the mission requirements.

3.1. Weight estimation and design lift coefficient

The ratio of W_e/W_{TO} can be obtained from historical data for general aircraft conceptual design. It can be easily stated that W_e/W_{TO} is about 0.85 [17]. One of the design requirements of the UAV is to carry a payload of 700 g weight. As W_e/W_{TO} ratio is about 0.85 at Eq. (1), then W_{TO}can be found as 4.67 kg.

$$(W_{TO} - 0.7)/W_{TO} = 0.85 \tag{1}$$

By considering the extra components and structures of VTOL systems, the initial take-off weight is determined as 4.7 kg.

Estimating the total weight allows the design lift coefficient to be found at the time of cruising, which is the design condition. The design lift coefficient is calculated which will lead the selection of the wing profile. For this purpose, considering the simple but most effective flight regime cruise conditions, the design lift coefficient corresponding to the lift force as well as the weight of the VTOL-FW UAV is calculated as 0.47 according to Eq. (2) [12]. The wing area of the VTOL-FW UAV is estimated to be 0.4 m^2 taking into account the competitors shown in Table 1 previously examined and listed. Cruise flight velocity is a mission requirement and it is given as 20 m/s.

$$W = L = 1/2\rho_{\infty}{V_{\infty}}^2 S_{wing} C_L \tag{2}$$

3.2. Airfoil selection

First of all, in order to select the right airfoil for the wing, design lift coefficient calculated in section 3.1 must be satisfied at a given angle of attack for any kind of airfoil. In addition, since the design lift coefficient is a relatively large value, the thickness of the wing profile to be selected must be high. At the same time, the low moment coefficient of the airfoil allows smaller stabilizers to be designed to provide longitudinal stability. For VTOL-FW UAV, options with low moment coefficient and thick profiles are presented in Fig. 2.

Reynolds number varies between 150,000 and 400,000 for UAVs with 5–8 kg take-off weight to evaluate the profiles given in Fig. 2 [18]. NACA 63-512, a = 0.4 of these mentioned profiles is chosen because it provides the design lift coefficient value of 0.47 at 1.1° angle of attack and gives relatively low moment coefficients. In addition, this profile is easy to manufacture since it has a nearly flat bottom. JavaFoil [19] is utilized to plot the change of lift and moment coefficients versus angle of attack for NACA 63-512, a = 0.4 at Fig. 3.

Please cite this article as: Ö. Dündar, M. Bilici and T. Ünler, Design and performance analyses of a fixed wing battery VTOL UAV, Engineering Science and Technology, an International Journal, https://doi.org/10.1016/j.jestch.2020.02.002

Table 1
VTOL UAVs from worldwide.

UAV	W_{TO} [kg]	Payload [kg]	S_{wing} [m^2]	Endurance [h]	AR
Alti Ascend	9	0.6	0.6	4	7
HeliPlane	8.5	1.6	0.68	1	9.7
KapetAir	6.5	1	1	1.5	11
DeltaQuad	6.2	1.2	0.9	2	6.2
Trinity	5	0.7	0.64	1.5	9
Trone	5	0.8	0.6	1.5	9
Kuzgun	4.7	0.7	0.44	0.42	9.2

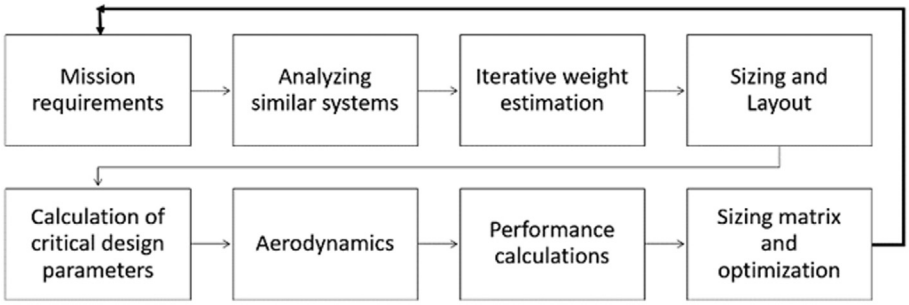

Fig. 1. The design methodology.

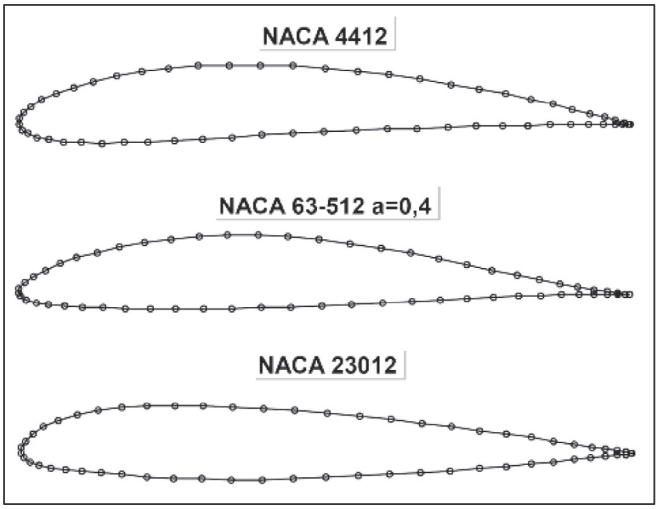

Fig. 2. NACA profiles options.

The fraction specified by "a" in NACA 63-512, a = 0.4 indicates the percentage of the airfoil chord over which the pressure distribution on the airfoil is uniform. It is selected as 0.4 to provide reduction in the drag by holding the pressure distribution at the middle of the airfoil. 6-digit NACA series is chosen for another reason that they give high maximum lift coefficient and very low drag over a small range of operation conditions such as Kuzgun VTOL-FW UAV [20].

3.3. Aspect ratio, wing sweep, taper ratio

For a tapered wing, the aspect ratio is defined as the span squared divided by the area [12]. The higher the aspect ratio, the bigger the maximum lift coefficient due to the portion of wing area that is not affected from tip vortices. Aspect ratio of VTOL-FW UAV is selected as big as possible to get rid of the vorticity near the tip of the wing. Aspect ratio of Kuzgun is determined as 9.2 to decrease the wing tip vortices considering the competitors.

Wing sweep is used primarily to reduce the adverse effects of transonic and supersonic flow. Theoretically, shock formation on a swept wing is determined not by the actual velocity of the air passing over the wing, but rather by the air velocity in a direction perpendicular to the leading edge of the wing. The wings will not be swept toward the front since there will be no high speeds effecting the aerodynamics of the Kuzgun. On the other hand, wing taper ratio, λ, is the ratio between the tip chord and the centerline root chord. Most wings of low sweep have a taper ratio of about 0.4–0.5 [12]. There are low wing tip vortices on account of low wing tip vortices so that Kuzgun uses 0.7 taper ratio which is slightly high compared to most used values. The advantage of using a relatively high taper ratio provides high lift compared to low taper ratio. Design parameters calculated and evaluated are summarized in Table 2.

4. Sizing of the wing and the control surfaces

In order for the wing to be dimensioned geometrically, firstly, the wing loading value is calculated. By calculating this value, the previously estimated real value of the wing area is actually found. By finding the wing area, detailed calculations of the wing and control surfaces are performed and designed. It is assumed that the total take-off weight of the VTOL-FW UAV remains constant in the calculations.

4.1. Wing loading

The wing loading is the weight of the aircraft divided by the area of the reference (not exposed) wing. Wing loading directly affects stall speed, climb rate, take-off and landing distances as well as turning performance. Also it determines the design lift coefficient, and impacts drag through its effect upon wetted area and wing span. There are many methods of calculating wing loading in aircraft designs according to the design requirements. In this study, stall speed and cruise speed are chosen as constraints in wing loading calculations. According to the two methods, the cal-

Please cite this article as: Ö. Dündar, M. Bilici and T. Ünler, Design and performance analyses of a fixed wing battery VTOL UAV, Engineering Science and Technology, an International Journal, https://doi.org/10.1016/j.jestch.2020.02.002

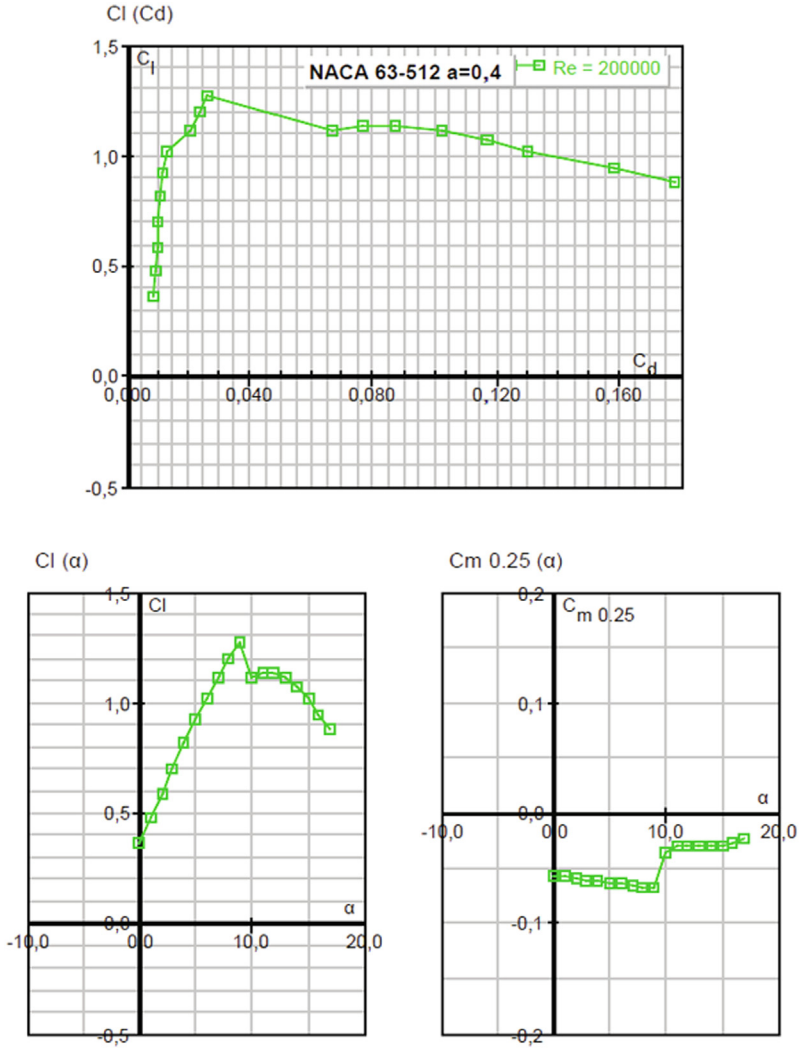

Fig. 3. NACA 63-512, a = 0.4 profile specifications at Re = 200,000.

Table 2
Design parameters of VTOL-FW UAV.

Parameter	Symbol	Value	Unit
Aspect Ratio	AR	9.2	–
Wing Span	b	2	m
Empty Weight	W_e	4	kg
Take-off Weight	W_{TO}	4.7	kg
Design Lift Coefficient	$C_{l,design}$	0.47	–
Cruise Speed	V_{cruise}	72	km/h
Taper Ratio	λ	0.78	–
Wing Twist	–	−1	Degree
Airfoil	–	NACA 63-512, a = 0.4	–

culations are made separately and the selection of the smaller value between the two values are made. The smallest value is chosen such that, if the wing is large enough to minimize the wing loading; it is highly possible that the wing will satisfy all other requirements [21].

4.1.1. Stall speed constraint

The stall speed of an aircraft is directly determined by the wing loading and the maximum lift coefficient. Stall speed is a major contributor to flying safety, with a substantial number of fatal accidents [12]. Wing loading from stall speed is calculated as Eq. (3).

$$W/S = 0.5\rho_{\infty}V_{stall}^{2}C_{L,max} \tag{3}$$

$$C_{Lmax} = 0.9 \times C_{l,max} \times \cos(\Lambda_{c/4}) \tag{4}$$

For a wing of fairly high aspect ratio (over about 5 or over), the maximum lift coefficient of whole aircraft ($C_{L,max}$) will be approximately 90% of the airfoil maximum lift coefficient ($C_{l,max}$) at the same Reynolds number, provided that the lift distribution is nearly elliptical [14].

4.1.2. Cruise speed constraint

During cruise flight, the lift equals the weight so that the lift coefficient equals the wing loading divided by the dynamic pressure. In the case of propeller aircraft, the transport coefficient changes in direct proportion to the square root of the drag factor [14]. At the same time, drag due to lift factor (K) value deals with the performance of the wing characteristics of the aircraft, and the growth of this value reduces aerodynamic performance. In addition, it is necessary to determine the drag coefficient that affects the entire VTOL-FW UAV to calculate the cruise speed requirement and wing loading. For this, the method given in Eq. (6) is found for all components of VTOL-FW UAV separately and zero lift drag coefficient is calculated. Expressions for cruise-speed constraint method are given in the Eqs. (5)–(7) respectively [12].

Please cite this article as: Ö. Dündar, M. Bilici and T. Ünler, Design and performance analyses of a fixed wing battery VTOL UAV, Engineering Science and Technology, an International Journal, https://doi.org/10.1016/j.jestch.2020.02.002

$$\frac{W}{S} = q_\infty \sqrt{\pi A R e C_{D_0}},\ C_L = \sqrt{\pi A R e C_{D_0}} = \sqrt{\frac{C_{D.0}}{3K}} \tag{5}$$

$$K = \frac{1}{\pi A R e} \ where\ e = 1.78\left(1 - 0.045AR^{0.68}\right) - 0.64 \tag{6}$$

$$C_{D_0} = \frac{\sum_i^n C_{fi} FF_i S_{wet,i}}{S_{ref,i}} + C_{D_{MR}} \tag{7}$$

In Eq. (5), K is drag-due-to-lift factor and e is Oswald efficiency factor demonstrating the efficiency of the wing. In Eq. (6), C_{fi} represents the skin friction coefficient of each component which is a strong function of Reynolds number, C_{D_0} is parasite drag of the whole UAV and $C_{D_{MR}}$ is drag coefficient of multi-rotor system. Skin friction coefficient can be found out through Eq. (8) supposing the fluid is turbulent everywhere in the flow field [12]. On the other hand, FF_i is the form factor that is an explanation of contribution of each component to the total drag. Finally, $S_{wet,i}$ and $S_{ref,i}$ are the wetted and reference areas respectively.

$$C_{f,turbulent} = \frac{0.455}{(logRe)^{2.58} x (1 + 0.144M^2)^{0.65}} \tag{8}$$

In order to calculate the parasite drag in detail, wetted areas and form factors are utilized as given at Table 3 [12]. Form factor increases in proportion with the thickness of the airfoil for the wing and control surfaces and the maximum diameter for the body. The most additive to parasite drag is provided by the wing due to its large wetted area. The need for extra volume of the rotor system, which realizes vertical take-off and landing, increases the size of the body. Therefore, the contribution of the body to the total drag is approximately 1/3 of the wing.

At Table 3, f is ratio of characteristic length which is generally selected as wing span or fuselage length divided diameter of the body. (t/c) represents the thickness ratio of the airfoil and Λ_m is the sweep angle of the wing. The induced-drag-coefficient at moderate angles of attack is proportional to the square of the lift coefficient with the drag-due-to-lift factor. Induced drag occurs by inducing the freestream velocity due to the vortexes in the wing arcs and its formula is given in Eq. (9). Induced drag is formed due to the lift itself by the vortex behind the wing inducing the freestream velocity to downwash another velocity vector.

In Fig. 4, the graphic of induced drag versus Mach number is given. As the speed increases, lift coefficient used to balance the weight of the VTOL-FW UAV decreases, the induced drag also decreases.

$$C_{D_i} = K\left(\frac{2W}{V_\infty^2 \rho_\infty S}\right)^2 \tag{9}$$

The left side of the formula in Eq. (6) represents the contribution of each component of the fixed-wing part of the UAV to drag, and the right side $(C_{D_{MR}})$ is the drag coefficient of the multi-rotor system that provides vertical landing and take-off. It is assumed that drag coefficient of the multi-rotor system is approximately equal to the all stopped propeller drag coefficient. The multi-rotor system, which provides vertical landing and take-off in Kuzgun, does not have a tilt mechanism, so it creates a steady flow resistance during cruise flight. Fig. 5 represents the shape of the side and plan views of the used Ramoser vario propeller. The surface area of the propeller while standing perpendicular to the flow is approximately the same as the surface area that it has when parallel to the flow as can be seen in Fig. 4. In this study, calculations are performed by accepting that the surface areas of side and plan propellers are the same for each case. This acceptance has reasonable results for propellers with small pitch values [22]. The drag coefficient of a stopped propeller standing against cruise flight is calculated using the formula in Eq. (10) [23]. Since the actual flight conditions always involve more compelling engagement, this calculated drag coefficient is multiplied by a correction factor to achieve more reliable results.

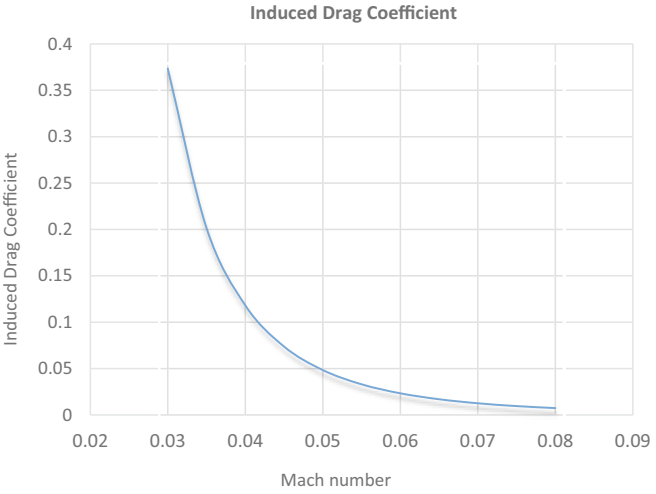

Fig. 4. Induced drag coefficient vs Mach number.

$$C_{D_{MR}} = \frac{0.1(NDC_{0.7R})}{S_{ref}} \tag{10}$$

The drag coefficients of the stopped propellers in the cruise flight are considerably higher. In Fig. 6 drag coefficient versus flight velocity of all stopped propellers are given. When there is no rotor system providing vertical landing and take-off, all drag coefficient consists of only zero-lift drag coefficient. However, adding the multi-rotor system, a drag coefficient up to zero-lift drag is added to the overall drag. In Fig. 6, it can be seen that the drag coefficient of multi-rotor system (all stopped propellers) is as same as zero lift drag coefficient which is 0.021. The reason of that drag increment of multi-rotor system comes mainly from disturbing the freestream air.

Wing loading calculations are summarized at Table 4. Among the two wing loading values, the smallest value is chosen such that if the wing is large enough to minimize the wing loading, it is highly possible that the wing will satisfy all other mission requirements [21].

Table 3
Parasite drag calculations.

Part	Form Factor (FF)	Wetted Area [m^2]
Body	$1 + \frac{60}{f^3} + \frac{f}{400}$	0.322
Wing	$\left[1 + \frac{0.6}{(\frac{t}{c})_m}\left(\frac{t}{c}\right) + 100\left(\frac{t}{c}\right)^4\right]\left[1.34M^{0.18}(\cos\Lambda_m)^{0.28}\right]$	0.821
V. tail		0.098
H. tail		0.121

Fig. 5. Side and plan views of propeller Ramoser vario.

Please cite this article as: Ö. Dündar, M. Bilici and T. Ünler, Design and performance analyses of a fixed wing battery VTOL UAV, Engineering Science and Technology, an International Journal, https://doi.org/10.1016/j.jestch.2020.02.002

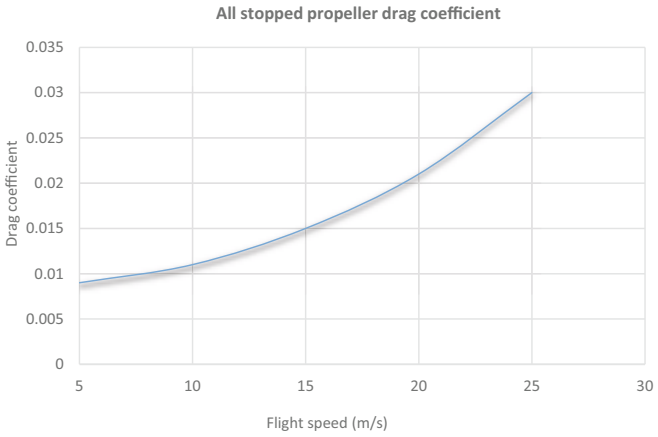

Fig. 6. All stopped propeller drag coefficient vs flight speed.

Table 4
Wing loading calculations.

Parameter	Symbol	Value	Unit
Stall speed	V_{stall}	53	km/h
Maximum lift coefficient	$C_{L,max}$	1.318	–
Wing loading-stall speed	$(W/S)_{stall\_speed}$	183.8	kg/ms^2
Oswald span efficiency	e	0.778	–
Skin friction coefficient	C_{f_e}	0.00615	–
Multirotor drag coefficient	$C_{D_{MR}}$	0.021	–
Parasite drag	C_{D_0}	0.0447	–
Wing loading-cruise speed	$(W/S)_{cruise\_speed}$	141.6	kg/ms^2

4.2. Sizing of the wing

Finding the wing loading value allows to determine the true value of the wing area. Actual wing area value is calculated as 0.485 m^2 for the wing loading value of 141.6 kg/ms^2 calculated for 4.7 kg take-off weight. Calculation of the wing area provides the determination of wing geometric characteristics such as wing root and tip chord length as well as average aerodynamic chord length with the selected taper ratio value in section 3.3.

$$c_r = \frac{2S_{wing}}{b(1+\lambda)} \tag{11}$$

$$c_t = \lambda c_r \tag{12}$$

$$\bar{c} = \frac{2}{3} c_r \frac{1+\lambda+\lambda^2}{1+\lambda} \tag{13}$$

Since Kuzgun travels at relatively low speeds, no sweep angle is given to the wing. Wing root chord length is calculated 0.272 m, tip chord length 0.21 m and mean aerodynamic chord length is 0.242 m. Since the biggest load on the wing is close to the root, the span is kept at the same root chord for 200 mm long of the wing.

4.3. Sizing of the control surfaces

For a front mounted propeller engine aircraft, historical trend shows that the tail moment arm of this type of the aircraft is generally between 0.6 and 0.7 [12]. Taking the horizontal tail volume ratio (V_{HT}) as 0.5 for a homebuilt aircraft [12] horizontal tail wing area and other specifications can be found out. For an arbitrary aircraft, a vertical tail has to be a little bit closer to the wing than the horizontal tail. This is to prevent the vertical tail to be masked by the wakes created by the horizontal tail. Therefore, with arbitrarily chosen value smaller than the moment arm value of the horizontal tail which is 0.57 is implemented [12]. In addition to this, vertical tail moment arm (V_{VT}) is 0.04 for homebuilt small UAVs [12].

Table 5
Wing and control surface sizing.

Parameter	Symbol	Value	Unit
Wing area	S_{wing}	0.485	m^2
Wing root chord	c_r	0.272	m
Wing tip chord	c_t	0.21	m
Mean aerodynamic chord	$\bar{c}$	0.242	m
Horizontal tail area	S_{HT}	0.07	m^2
Horizontal tail moment arm	S_{VT}	0.66	m
Vertical tail area	l_{HT}	0.055	m^2
Vertical tail moment arm	l_{VT}	0.627	m

$$V_{HT} = \frac{l_{HT}S_{HT}}{\bar{c}S} \tag{14}$$

$$V_{VT} = \frac{l_{VT}S_{VT}}{bS} \tag{15}$$

Wing and control surface sizing parameters in detail are represented in Table 5.

5. Performance calculations

The most challenging complexity of electrical battery powered VTOL-FW UAV is underestimating the power required for take-off and especially transition from hover to cruise flight [1]. Since the VTOL-FW UAVs can perform vertical landing and take-off, the total take-off weights are higher than the fixed-wing UAVs of the same dimensions, as they require equipment such as extra motors, mechanisms, servo motors and propellers. This situation consumes extra power, especially due to excessive work done against gravity at the time of vertical take-off. In addition, complex aerodynamic interactions disrupt the flow pattern during the transition from the hover position to the cruise flight, causing excessive energy spent. As a result, compared to UAVs of similar sizes, VTOL-FW UAVs have shorter flight times due to the enormous amount of energy they spend.

Kuzgun's performance is examined by calculating the maximum and required powers, determining the energy consumption for each flight condition, and comparing the battery's model with the identified parameters in Simulink and comparing them with standard solutions.

5.1. Maximum power

T/W is the ratio of the thrust of the UAV to the weight and directly affects the performance. An UAV with a higher T/W will accelerate more quickly, climb more rapidly, reach a higher maximum speed as well as sustain higher turn rates. However, higher the thrust, higher the weight of the motor. In addition, T/W is not a constant, it varies with altitude and velocity as well as the horsepower and propeller efficiency. For an UAV, Eq. (16) [12] is used to calculate maximum power by using some design parameters and maximum speed.

$$P_{max}/W = a \times V_{max}^{c} \text{ where } a = 0.004,\ c = 0.57 \tag{16}$$

5.2. Power required calculations

Power requirements are the primary parameters that affect VTOL-FW UAV design the most. Power calculations significantly affect battery selection and thus take-off weight. Besides, the low

Please cite this article as: Ö. Dündar, M. Bilici and T. Ünler, Design and performance analyses of a fixed wing battery VTOL UAV, Engineering Science and Technology, an International Journal, https://doi.org/10.1016/j.jestch.2020.02.002

amount of power required has positive effects on the flight time and range of the VTOL-FW UAV. Battery energy is consumed by doing a great deal of work, especially during vertical take-off. There are also great power requirements at the time of climbing, but since the climbing flight is short-term, battery energy consumption is relatively low for the climbing flight. In the cruise flight, calculations are made on the remaining battery energy from other flight conditions. The more battery energy is left, the longer the endurance of VTOL-FW UAV. In this study, power requirements are calculated and energy consumption for every flight condition is simulated by using Simulink for the selected battery.

5.2.1. Power required for cruise

Power required for cruise can be found from multiplication of cruise speed and thrust required. Thrust required is directly equal to the drag at cruise conditions and given in Eq. (17) [14].

$$P_{cruise} = VT_{cruise} \; where \; T_{cruise} = D = q_{\infty} S C_D \tag{17}$$

5.2.2. Power required for take-off

The power required of rotorcraft can be derived based on momentum theory on rotor disk [24]. In order to realize vertical take-off and landing the ratio of thrust to weight K_T needs to be greater than one. The maximum design power and thrust required of the VTOL-FW UAV can be written as Eqs. (18) and (19) respectively [25].

$$P_{TO} = \frac{T_{TO} V_{TO}}{2} \left[\sqrt{1 + \frac{2T_{TO}}{\rho_{\infty} {V_{TO}}^2 A_{prop}}} \right] \tag{18}$$

$$T_{TO} = K_T W_{TO} \tag{19}$$

In Eq. (14), K_T is the ratio of thrust to weight at take-off condition and is selected as 1.2 for small VTOL UAV concept since Stone [26] suggests that the maximum thrust needs to be 1.15 or higher times greater than takeoff weight, for dealing with non-ideal conditions and transition maneuvers.

5.2.3. Power required for climbing

While thrust in cruise is simply given by the correspondent drag, for climb it is determined using the constant rate of climb, defined as a specific mission requirement. The required power at the moment of climbing is found by multiplying the sum of the vertical component, whose weight depends on the angle of climb, and the drag force, by the speed of the climb [27]. φ is the climb angle and power required for climb is given simply in Eq. (20).

$$\begin{aligned} P_{climb} &= \left[W sin(\varphi) + C_D q_{\infty} S_{wing} \right] V_{climb} \\ V_{climb} &= 1.2 \sqrt{\frac{2W}{S_{wing} \rho_{SL} C_{L\,max}}} \end{aligned} \tag{20}$$

5.2.4. Power required for landing

Being subjected to structural constraints and landing quality requirements, the landing velocity of a VTOL-FW UAV should be strictly restricted. In axial descend case, axial climb model is not valid anymore since the rotor disk works in vortex ring state that exist for the case of descent velocity is less than two times of hover induced velocity. Consequently, landing required power must be lower than power required for take-off [23]. The induced velocity V_H at the propeller disk in hover is an important reference for the analysis of VTOL-FW UAV descent, which could be expressed in Eq. (16). A descent velocity of V_{Des} = 4 m/s was suggested in this paper, and then the propellers are working on a condition of low speed axial descent $V_{Des} < 2V_H$. Assuming the variable $x = -V_{Des}/V_H$, the actual induced velocity V_i at the propeller disk can be given by the quartic approximation given in Eq. (21) [25].

$$V_H = \sqrt{\frac{T_{hover}}{2\rho_{SL} A_{prop}}}$$

$$V_i = (\mathrm{K} - 1.125x - 1.372x^2 - 1.718x^3 - 0.655x^4) V_H \tag{21}$$

In landing all aerodynamic effects on the wing is ignored due to lack of cruise flight. The power required of each propeller at such low rate of descent can be expressed as:

$$P_{landing} = KW_{TO}(V_i - V_{Des}) \tag{22}$$

5.3. Energy consumption

Lithium Polymer (Li-Po) battery provides the energy needed for power requirements in every flight condition. The calculated required power quantities are valid for one hour of usage. However, flight times in all different conditions are limited to minutes. The take-off time of VTOL-FW UAV to 300 m altitude is 1.5 min, the climbing time is 30 seconds and the landing time is 50 seconds. The energy consumption to be withdrawn from the battery will increase as the take-off time will increase for higher altitude flights.

The required power values for different flight conditions can be converted into electrical energy (Wh) considering the flight times by taking subsystem efficiency into account. System thrust causing energy consumption in VTOL-FW UAV. The propulsion components consist of propeller, rotor, motor, and electronic speed control (ESC) unit. All propulsion system components take their energy from the battery in direct proportion to the time they use it. However, there are losses in the transmission of energy from the battery due to cables and mechanical reasons. The essential element causing the propulsion is the propeller, but until the power transmission reaches the propeller, it passes many elements as shown in Fig. 7. Losses in flight control card, ESC and engine are high so that it cannot be neglected. The inclusion of losses in the calculations is carried out with efficiency rates and equations for these efficiencies are given in Eqs. (23) and (24) respectively.

$$\eta_{cruise} = \eta_{prop} * \eta_{motor} * \eta_{esc} \tag{23}$$

$$\eta_{multirotor} = FM * \eta_{motor} * \eta_{esc} \tag{24}$$

FM is called figure of merit which is equivalent to static thrust efficiency and defined as the ratio of the ideal power required to hover to the actual power required. It is selected as 0.7 which is ideal for mini UAVs and considered as constant through all flight conditions [28]. Propeller efficiency is generally accepted as 0.8 according to several studies [29,30]. ESC efficiency is affected by resistive losses in electronics due to duty cycle. At normal operation condition as cruise which often set the throttle level around 40% to 60%, within this range the efficiency is drop from nearly 1 to 100% duty cycle to 0.85–0.9 [1]. Therefore, the efficiency can be chosen 0.85 for ESC [31]. Finally, motor is assumed to be 0.9 efficiency [32,33]. The efficiencies for the evaluated parameters are given at Table 6.

The selected battery has 20,000 mAh 22.2 V with 6 cells that leads to 444 Wh consumable energy. In order to find out the total endurance of Kuzgun, take-off, climb and landing energy consumptions are calculated so that rest of energy for cruise could be determined. In Table 7, energy consumption for every flight condition formulation is given. A little portion of battery energy is used for climb and landing while take-off consumes much higher energy. It is crystal clear from Table 7, the rest of the energy from battery for cruise is 405.9 Wh. However, this value is corrected by a factor that is necessary for other electronic energy provided from battery.

Please cite this article as: Ö. Dündar, M. Bilici and T. Ünler, Design and performance analyses of a fixed wing battery VTOL UAV, Engineering Science and Technology, an International Journal, https://doi.org/10.1016/j.jestch.2020.02.002

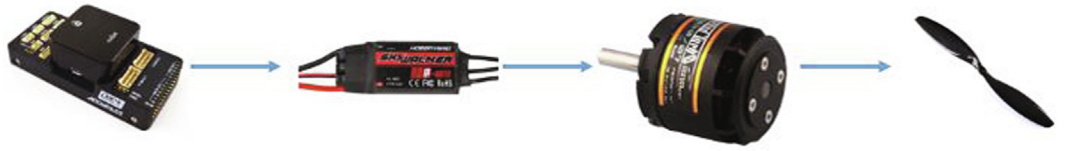

Fig. 7. Conversion of battery power to available propulsive power.

Table 6
Propulsive system parameter efficiencies.

Parameter	Value
Propeller efficiency	0.8
Motor efficiency	0.9
ESC efficiency	0.85
Figure of merit	0.7
Total efficiency for cruise	0.65
Total efficiency for multi-rotor	0.57

Table 7
Simulation results.

Flight condition	Flight duration [s]	Energy consumption [Wh]	Energy consumption [Wmin]
Take off	90	19.7	1182
Climbing	30	6.3	378
Landing	50	12.1	726
Cruise	1330	405.9	24354

5.4. Battery model

Energy is one of the indispensable needs of today. The world provides most of its energy needs from traditional energy sources such as natural gas, oil as well as coal. With the rapidly increasing world population, the demand for energy and the electronic devices becoming portable, the need for batteries has increased tremendously in all areas of life. Batteries, which convert chemical energy into electrical energy and store it within its body, are produced in many different types and features due to the variety of usage areas.

The basic electrochemical unit in batteries is called as "cell". The battery is connected in parallel or in series, depending on the appropriate capacity and output voltage or it contains cells that are connected in two ways. Although daily or disposable batteries are low in power and capacity, they are small in size and advantageous in terms of portability. Depending on whether the batteries are recharged or not, they are divided into two parts: primary battery and secondary battery [34]. Secondary batteries are batteries that can reproduce electrical energy after discharge. After the battery is discharged, electric current is applied in the opposite direction of the current and the battery is recharged. Zinc-carbon, alkaline, zinc-silver, zinc-air, mercury oxide are examples of primary batteries, lead-acid, nickel-cadmium, nickel-metal-hydride, lithium-ion, lithium polymer are examples of secondary batteries [34]. Voltage, capacity, energy, specific energy and energy density, self-discharge, number of cycles, temperature are the performance criteria of batteries [35]. These types of batteries are preferred due to their long lifetime, affordability and they can be used by recharging between 500 and 1000 times on average.

Lithium-Ion (Li-Ion)/Lithium-Polymer (Li-Po) batteries are considered as high-capacity batteries, which can be designed for either high energy or high power applications. They are generally used for mini-UAVs as energy producer. While there is a need for a model capable to describes the battery behavior, with a variation of battery conditions such as state of charge (SoC), temperature, current rates, loading conditions static or dynamic loading and its applications [36].

In this study, 22.2 V 20,000 mAh Lithium-Polymer (Li-Po) battery is used as energy producer. The battery is modelled in MATLAB Simulink environment. Simplified block diagram of the battery model is shown in Fig. 8. Changes of state of charge, current and

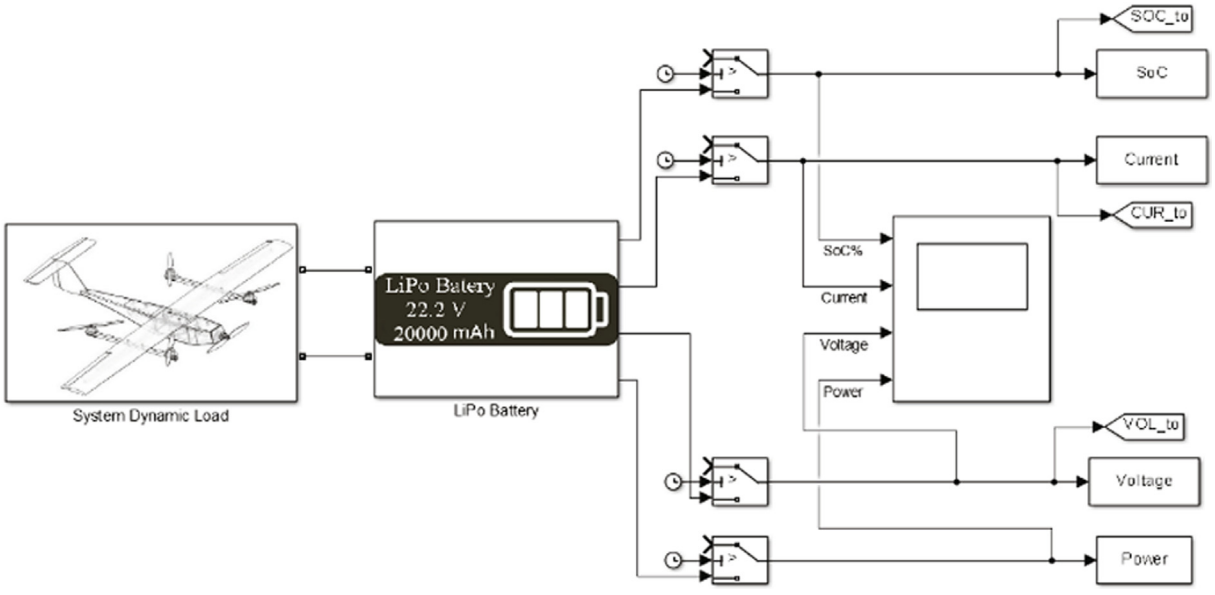

Fig. 8. General Simulink view of battery model.

Please cite this article as: Ö. Dündar, M. Bilici and T. Ünler, Design and performance analyses of a fixed wing battery VTOL UAV, Engineering Science and Technology, an International Journal, https://doi.org/10.1016/j.jestch.2020.02.002

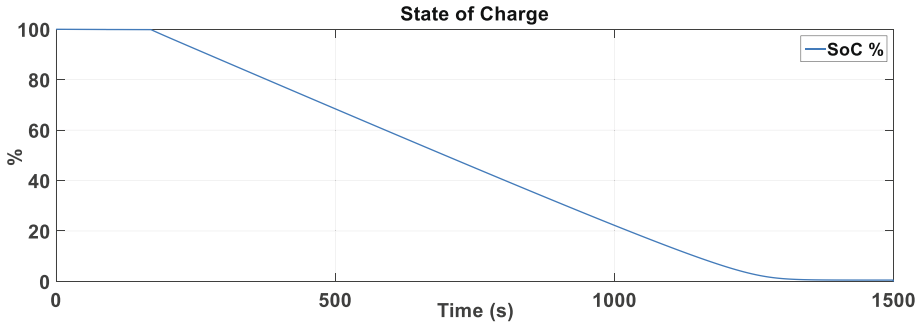

Fig. 9. State of charge of battery in missions.

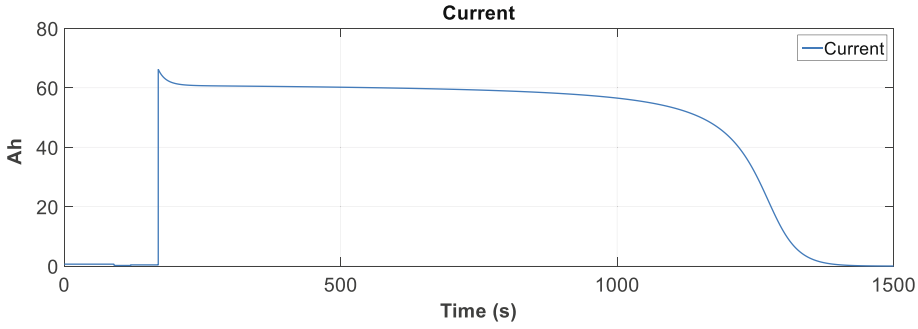

Fig. 10. Necessary current in missions.

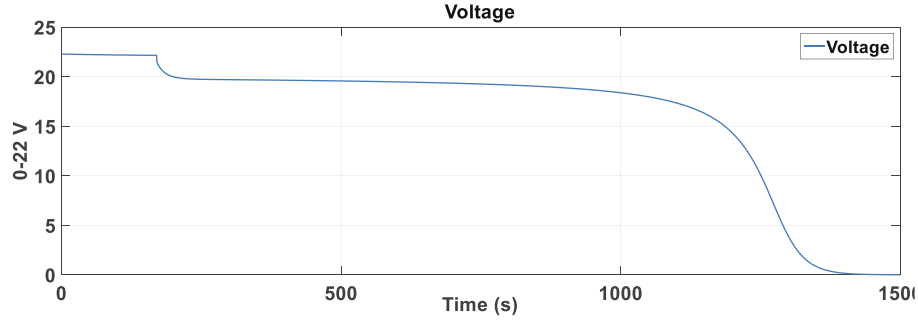

Fig. 11. Voltage changing in the system during the flight.

voltage with respect to time are represented in Fig. 9, Fig. 10 and Fig. 11, respectively.

Dynamic loads are modelled respectively for these phases: take-off, climbing, landing, and cruise. Missions durations covers 90 seconds for take-off, 30 seconds for climbing, 50 seconds for landing, and rest of the battery capacity is for cruise. Duration of the flight is calculated as about 1500 seconds (25 minutes). This flight time is an acceptable one compared to real systems using 20,000 mAh Li-Po battery [37].

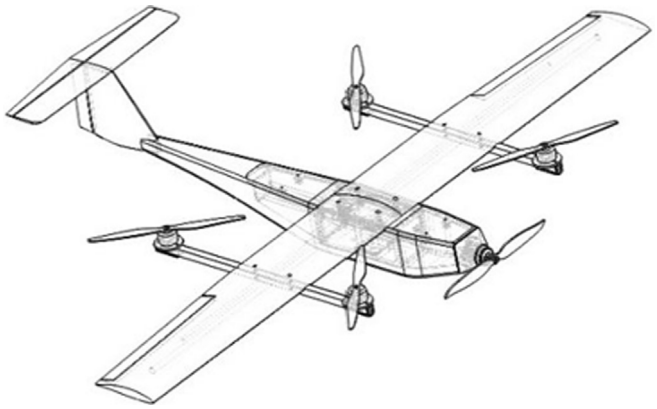

Fig. 12. General view of Kuzgun.

6. Results and discussion

VTOL-FW UAV that is accomplished to design have an ability to do vertical take-off and landing with its four vertical and one horizontal engines. It has 4.7 kg total take-off weight, 2 meters long wing span and is able to fly at maximum fineness ratio with 72 km/h cruise speed. General perspective view of VTOL UAV designed is shown at Fig. 12.

Table 8
Parasite drag coefficients and endurance values for FW only and VTOL-FW.

Fixed wing drag coefficient	$\frac{S_{wet}}{S} C_{fe}$	0.0206
Multirotor system drag coefficient	$C_{D_{MR}}$	0.021
Fixed wing endurance	E_{range_fw}	45 min
Fixed wing with multi-rotor system endurance	E_{range_mr}	25 min

Please cite this article as: Ö. Dündar, M. Bilici and T. Ünler, Design and performance analyses of a fixed wing battery VTOL UAV, Engineering Science and Technology, an International Journal, https://doi.org/10.1016/j.jestch.2020.02.002

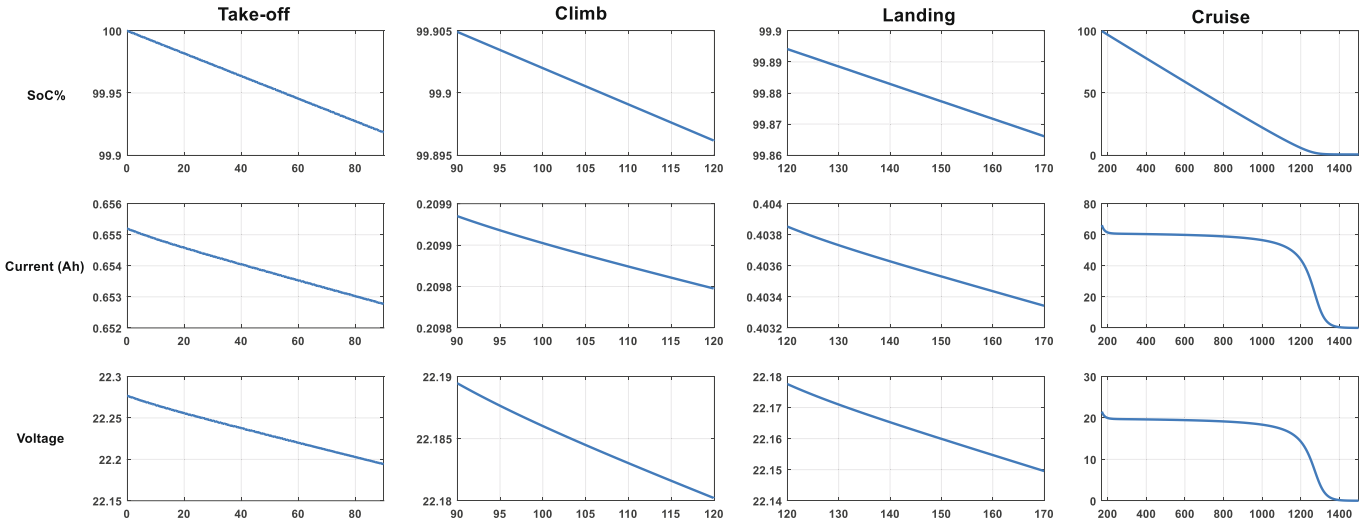

Fig. 13. General results during missions.

The first goal of design is to decrease take-off weight and maximize the endurance as much as possible. In order to achieve this aim, high aspect ratio value is selected to get rid of the tip vortices along the wing area. Aerodynamic calculations and geometric dimensions are performed to reach the maximum efficiency. In order to evaluate the power and energy results 20,000 mAh 6S 22.2 V LiPo battery having 444 Wh consumable energy is chosen to fulfill mission endurance requirement. Battery model is performed in MATLAB Simulink by using power requirements for different kinds of flights including take-off, climbing, landing as well as cruise. Simulation results show that vertical take-off consumed 4.4%, landing consumed 2.7% and climbing consumed 1.4% energy of battery. Therefore cruise endurance is found out as 1330 seconds (22.1 minutes) which fulfills the mission requirement. In unaccelerated level flight, drag increased dramatically with presence of four vertical engine and its propellers than expected.

Table 8 shows the difference between the drag coefficients of only fixed wing (FW) and multi-rotor system (fixed wing + multi-rotor engines and propellers). Increment of parasite drag in level flight due to the four engines and propellers results in substantially decrement of endurance. In Fig. 13, general results from Simulink during different mission conditions are represented.

7. Conclusion

In this study, design and performance analysis of a VTOL-FW UAV having four propeller-multi-rotor system with the ability of vertical take-off and landing is performed. First of all, the geometric and aerodynamic design of the VTOL-FW UAV is done for low drag and high lift coefficient to minimum the power required hence maximum the endurance. The battery selection is conducted for the 4.7 kg take-off weight and 2 meters long wing span VTOL. While competitors with these geometric dimensions utilize high-tech batteries, Kuzgun is experienced with a battery that is easy to access and cheap, such as Li-Po. Power required for every mission including cruise flight, take-off, climbing and landing is calculated. Selected battery is modelled with Simulink to represent energy consumption for every flight conditions. The rest of the energy value of the battery is determined from the energy consumption values for different kind of flight conditions. Hereby, the endurances are found out for given mission requirements.

It is showed that four propellers providing vertical take-off and landing as well as hovering increase the total drag. This situation results in the decrement of endurance. In addition, transition from hovering to cruise dramatically reduces the energy of battery. In conclusion, it is highly logical to use VTOL-FW UAV concept for hilly and forested areas especially if there is no need for long endurance. In future work, manufacturing and flight tests of Kuzgun will be performed. The main production method will be three-dimensional printer (3D printer) technology with the material polylactic acid (PLA) reinforced with carbon-fiber. On the other hand, energy consumption and power values will be checked to verify the simulation results by using suitable sensors on Kuzgun at real fight tests.

Declaration of Competing Interest

The authors declare that they have no known competing financial interests or personal relationships that could have appeared to influence the work reported in this paper.

References

[1] B. Yuksek, A. Vuruskan, U. Ozdemir, A. Yukselen, G. Inalhan, Transition flight modeling of a fixed wing VTOL UAV, J. Intell. Rob. Syst. 84 (1–4) (2016) 83–105, https://doi.org/10.1007/s10846-015-0325-9.
[2] Daeil Jo, Yongjin Kwon, Analysis of VTOL UAV propellant technology, J. Comput. Commun. 5 (2017) 76–82, https://doi.org/10.4236/jcc.2017.57008.
[3] Adnan S. Saeed, Ahmad Bani Younes, Shafiqul Islam, Jorge Dias, Lakmal Seneviratne, Guowei Cai, A review on the platform design, dynamic modeling and control of hybrid UAVs, in: Int. Conference on Unmanned Aircraft Systems (ICUAS) 2015, Colorado, USA, https://doi.org/10.1109/ICUAS.2015.7152365.
[4] E. Çetinsoy, E. Sırımoğlu, K.T. Öner, C. Hançer, M. Ünel, Design and development of a tilt-wing UAV, Turk. J. Elec. Eng. Comp. Sci. 19 (5) (2011) pp, https://doi.org/10.3906/elk-1007-621.
[5] Aws Abdulsalam Najm, Ibraheem Kasim Ibraheem, Nonlinear PID controller design for a 6-DOF UAV quadrotor system, Eng. Sci. Technol., Int. J. (2019). https://doi.org/10.1016/j.jestch.2019.02.005.
[6] U. Ozdemir, Y. Aktas, A. Vuruskan, Y. Dereli, A. Tarhan, K. Demirbag, A. Erdem, G. Kalaycioglu, I. Ozkol, G. Inalhan, Design of a commercial hybrid VTOL UAV system, J. Intell. Rob. Syst. 74 (1–2) (2014) 371–393, https://doi.org/10.1007/s10846-013-9900-0.
[7] Yu. Seunghee, J. Heo, S. Jeong, Y. Kwon, Technical analysis of VTOL UAV, J. Comput. Commun. 04 (15) (2016) 92–97, https://doi.org/10.4236/jcc.2016.415008.
[8] J.P. Campbell, Research on VTOL and STOL aircraft in the United States, in Advances in Aeronautical Sciences: Proceedings of the first International Congress in the Aeronautical Sciences, vol. 2. Pergamon Press, 1959.
[9] URL: http://cargocopter.be/blog.html (2016).
[10] M. Aksugur, G. Inalhan, Design methodology of a hybrid propulsion driven electric powered miniature tailsitter unmanned aerial vehicle, J. Intell. Rob. Syst. 57 (1–4) (2010) 505–529, https://doi.org/10.1007/s10846-009-9368-0.

Please cite this article as: Ö. Dündar, M. Bilici and T. Ünler, Design and performance analyses of a fixed wing battery VTOL UAV, Engineering Science and Technology, an International Journal, https://doi.org/10.1016/j.jestch.2020.02.002

[11] Giovanni Droandi, A. Zanotti, G. Gibertini, Aerodynamic interaction between rotor and tilting wing in hovering flight condition, J. Am. Helicopter Soc. 60 (4) (2015), https://doi.org/10.4050/JAHS.60.042011.
[12] Daniel P. Raymer, Aircraft Design: A Conceptual Approach, fifth ed., Conceptual Research Corporation Sylmar, California, 1970.
[13] M.N. Kaya, F. Kose, D. Ingham, L. Ma, M. Pourkashanian, Aerodynamic performance of a horizontal axis wind turbine with forward and backward swept blades, J. Wind Eng. Ind. Aerodyn. 176 (2018) 166–173.
[14] John D. Anderson Jr, 2010. Aircraft Performance and Design, McGraw-Hill.
[15] Quick, D., Israel Aerospace Industries Unveils Tiltrotor Panther UAV Platform, AERO GIZMO, 2010.
[16] Frost and Sullivan: Study Analysing the Current Activities in the Field of UAV. European Commision, ENTR/2007/065, 2007.
[17] K.M. Tint, T.S. Win, Range and payload trades study on aircraft conceptual design, Int. J. Res. Publ. 20 (1) (2019).
[18] Sharma Hemant, Roshan Suraj, Antony, G. Ramesh, Ahmed Sajeer, Narayan Prasobh, Design of a high altitude fixed wing mini UAV – aerodynamic challenges. In: ICIUS 2013, 25 Sep 2013, Jaipur.
[19] Javafoil, https://www.mh-aerotools.de/airfoils/javafoil.htm.
[20] W.A. Timmer, An overview of NACA 6-digit airfoil series characteristics with reference to airfoils for large wind turbine blades. 47th AIAA Aerospace Sciences Meeting Including the New Horizons Forum and Aerospace Exposition, 5-8 January 2009, Orlando, Florida.
[21] E. Turanoguz, N. Alemdaroglu, Design of a medium range tactical UAV and improvement of its performance by using winglets, 2015 International Conference on Unmanned Aircraft Systems (ICUAS), 2015, doi: 0.1109/ICUAS.2015.7152399.
[22] P. Burgers, A thrust equation treats propellers and rotors as aerodynamic cycles and calculates their thrust without resorting to the blade element method. Int. J. Aviat. Aeronaut. Aerosp. 6 (5) (2019).
[23] W. Saengphet, C. Thumthae, Conceptual design of AED transport VTOL, in: The 7th TSME International Conference on Mechanical Engineering, 2016.
[24] Gordon J. Leishman, Principles of Helicopter Aerodynamics, second ed., Cambridge University Press, New York, NY, USA, 2006, p. 2006.
[25] , Int. J. Aerosp. Eng. 2016 (2016) 1–11, https://doi.org/10.1155/2016/3570581.
[26] R.H. Stone, The T-wing tail-sitter unmanned air vehicle: from design concept to research flight vehicle, Proc. Inst. Mech. Eng., Part G: J. Aerosp. Eng. 218 (6) (2004) 417–433.
[27] L.W. Traub, Range and endurance estimates for battery-powered aircraft. J. Aircr. 48 (2) (2011) 703–707. doi: 10.2514/1.C031027.
[28] M. Gatti, F. Giuletti, M. Turci, Maximum endurance for battery-powered rotary-wing aircraft, Aerosp. Sci. Technol. 45 (2015) 174–179.
[29] , Int. J. Aerosp. Eng. 2018 (2018) 1–23, https://doi.org/10.1155/2018/5782017.
[30] A. Manchin, W.M. Lafta, D.Z. Dao, Smart variable pitch propeller system for unmanned aerial vehicles, Int. J. Eng. Technol. 7 (4) (2018) 5238–5241, https://doi.org/10.14419/ijet.v7i4.21199.
[31] A. Gong, D. Verstrete, Experimental testing of electronic speed controllers for UAVs, 53rd AIAA/SAE/ASEE Joint Propulsion Conference (2017), https://doi.org/10.2514/6.2017-4955.
[32] B. Saha, E.T. Koshimoto, C. Chi Quach, E.F. Hogge, T.H. Strom, B.L. Hill, S.L. Vazquez, Kai F. Goebel, Battery health management system for electric UAVs, 2011 IEEE Aerospace Conference Proceedings (2011), https://doi.org/10.1109/AERO.2011.5747587.
[33] O. Gur, A. Rosen, 12th AIAA/ISSMO Multidisciplinary Analysis and Optimization Conference, 2018. doi: 10.2514/6.2008-5916.
[34] İ. Karaaslan, Poli(Hema-Ko-Mma) Tabanlı Lityum-Polimer Elektrolitlerin Sentezi, Karakterizasyonu Ve Uygulamaları, Master Thesis, Kocaeli University, 2019.
[35] M. Kaynak, Lityum Polimer Pillerde Kullanım Amaçlı Lityum İyon İletken Nanokompozit Elektrolitlerin Sentezi ve Karakterizasyonu, Master Thesis, Fatih University, 2015.
[36] Mohamed Daowd, Battery models parameter estimation based on Matlab/Simulink, The 25th World Battery, Hybrid and Fuel Cell Electric Vehicle Symposium & Exhibition, Shenzhen, China, Nov. 5–9, 2010.
[37] G. Hadi, A. Budiyarto, Design of separate lift and thrust hybrid unmanned aerial vehicle, J. Instrum. Autom. Syst. 2 (2) (2015).

Please cite this article as: Ö. Dündar, M. Bilici and T. Ünler, Design and performance analyses of a fixed wing battery VTOL UAV, Engineering Science and Technology, an International Journal, https://doi.org/10.1016/j.jestch.2020.02.002